

Supporting Information

A diketopyrrolopyrrole–based fluorescence turn–on probe for the detection of Pb²⁺ in aqueous solution and living cells

Xiaofeng Yang ^{a,b,*}, Yan Zhang^a, Yexin Li ^a, Xiaolei Liu ^a, Jiaxin Mao ^a, Yuan Yuan ^a, Yu Cui ^{a,*},

Guoxin Sun ^a, Guangyou Zhang ^a

^a School of Chemistry and Chemical Engineering, University of Jinan, No. 336, West Road of Nan Xinzhuang, Jinan 250022, Shandong, China

^b Shandong Provincial Key Laboratory of Fluorine Chemistry and Chemical Materials, University of Jinan, No. 336, West Road of Nan Xinzhuang, Jinan 250022, Shandong, China

CONTENTS:

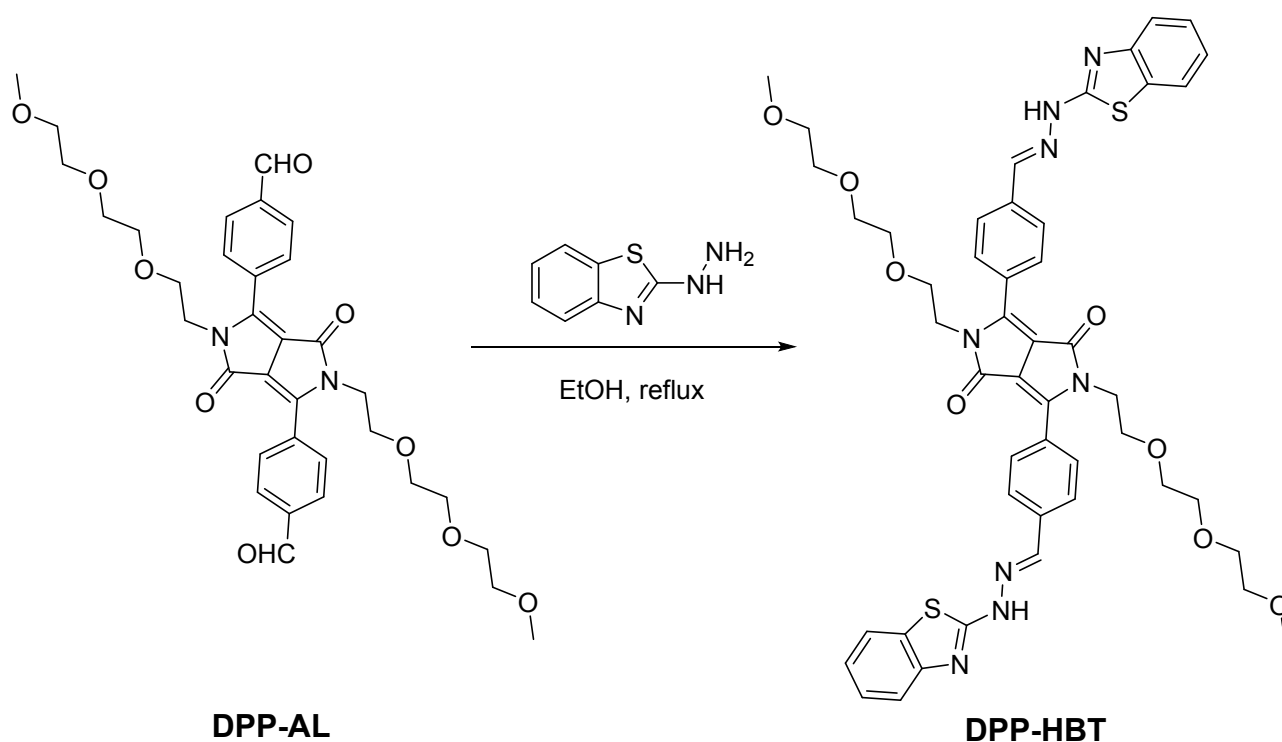
1. General information
2. Synthesis section
3. Cell imaging
4. Absorption spectra of **DPP–HBT** with Pb²⁺
5. Job's plot for the **DPP–HBT** and Pb²⁺
6. Binding constants between probe **DPP–HBT** and Pb²⁺
7. Determination of detection limit of Pb²⁺
8. Time-dependent fluorescence changes of **DPP–HBT** with Pb²⁺
9. The fluorescence intensity changes of **DPP–HBT** in the presence of Pb²⁺ ions and EDTA
10. Effect of pH
11. Cytotoxicity assay of **DPP–HBT**
12. ¹H and ¹³C NMR of **DPP–HBT**
13. Comparison of the present probe **DPP–HBT** and already available Pb²⁺ probes

Experimental Section

1. General Methods:

2-Hydrazinobenzothiazole was purchased from Aladdin Shanghai Reagent Company. Other reagents were used without further purification. Reactions were monitored by TLC. Flash chromatography separations were carried out using silica gel (200-300 mesh). ^1H NMR and ^{13}C NMR spectra were collected on a Bruker Avance II 400 MHz spectrometer. UV-vis spectra were recorded on a Shimadzu 3100 spectrometer. Fluorescence measurements were carried out using an Edinburgh Instruments Ltd-FLS920 fluorescence spectrophotometer.

2. Synthesis Section



Scheme S1. Synthetic route of **DPP-HBT**

Probe **DPP-HBT** was prepared according to the method we reported previously by a simple reaction of 4,4'-(2,5-bis(2-(2-(2-methoxyethoxy)ethoxy)ethyl)-3,6-dioxo-2,3,5,6-tetrahydropyrrolo[3,4-c]pyrrole-1,4-diyl)dibenzaldehyde (**DPP-AL**) and 2-hydrazinobenzothiazole^[1]. To 20 mL of compound **DPP-AL** (318 mg, 0.5 mmol) in ethanol, was added 5 mL of 2-hydrazinobenzothiazole (182 mg, 1.1 mmol) in ethanol dropwise. After the reaction solution was refluxed for 3 h, the rust red solid was precipitated, collected, and wash with ethanol to afford compound **DPP-HBT** (302 mg, 65%). ^1H NMR (DMSO- d_6 , 400 MHz) δ (ppm) 12.56 (br, 2H), 8.22 (s, 2H), 8.04 (d, $J = 8.4$ Hz, 4H), 7.87 (d, $J = 8.4$ Hz, 4H), 7.79 (d, $J = 4.8$ Hz, 2H), 7.46 (d, $J = 4.8$ Hz, 2H), 7.32 (t, $J = 8.0$ Hz, 2H), 7.14 (t, $J = 7.2$ Hz, 2H), 3.92 (t, $J = 6.0$ Hz, 4H), 3.56 (t, $J = 6.0$ Hz, 4H), 3.41-3.36 (m, 16H), 3.18 (s, 6H). ^{13}C NMR (DMSO- d_6 , 100 MHz) δ (ppm) 167.73, 162.28, 148.28, 137.36, 133.52, 130.16, 130.03, 129.37, 128.69, 127.02, 126.56, 122.35, 122.07, 109.62, 71.74, 71.70, 70.30, 70.09, 68.43, 68.37, 58.50, 42.01; HRMS-ESI: m/z calcd (%) for $\text{C}_{48}\text{H}_{51}\text{N}_8\text{O}_8\text{S}_2$: 931.3271 [M+H]⁺; Found: 931.3242; Element analysis for $\text{C}_{48}\text{H}_{50}\text{N}_8\text{O}_8\text{S}_2$ (%): C 61.88, H 5.37, N 12.14, calculated C 61.92, H 5.41, N 12.03 (Fig. S9).

References

[1] X. Yang, G. Zhang, Y. Li, Z. Liu, X. Gong, B. Gao, G. Zhang, Y. Cui, G. Sun, Colorimetric and fluorogenic signalling of fluoride ions by diketopyrrolopyrrole-based chemosensor, *RSC Adv.* 5 (2015) 22455–22462.

3. Cell Imaging

A549 Human Lung Adenocarcinoma cell lines were grown in DMEM supplemented with 10% FBS (fetal bovine serum) in an atmosphere of 5 % CO₂ at 37 °C. The cells were plated on 12 mm cover glasses in 6-well plate and allowed to grow for 24 h. Before the experiments, the cells were washed with PBS buffer, and then the cells were incubated **DPP–HBT** (10 μM) for 20 min at 37 °C then washed with PBS three times. After incubating with Pb²⁺ (20 μM) for 30 min at 37 °C, cells were rinsed with PBS three times. Then, the fluorescence images were acquired through an Olympus IX71 fluorescence microscope.

4. Absorption spectra of DPP–HBT with Pb²⁺

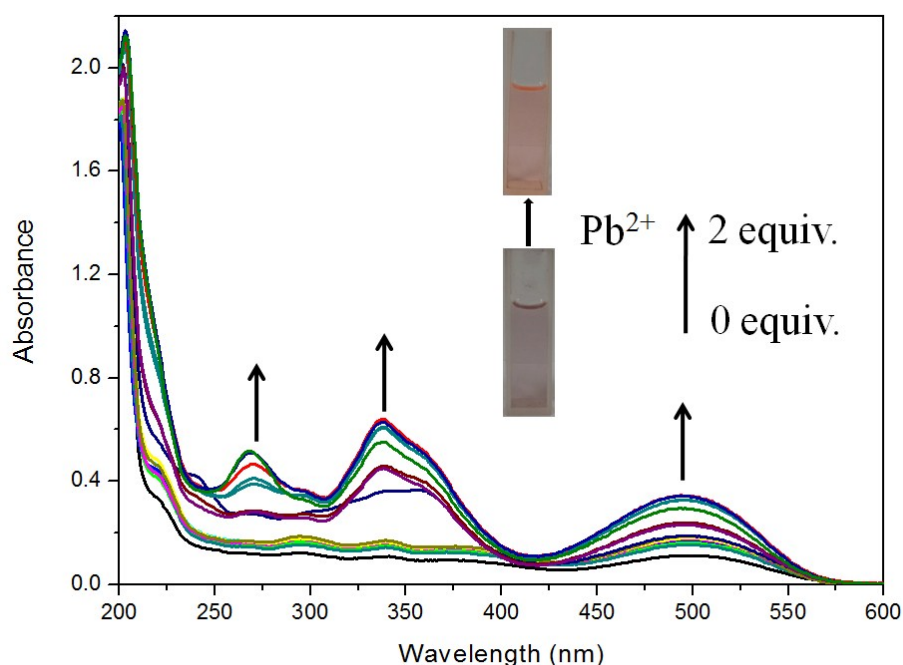


Figure S1. Absorption spectra of **DPP–HBT** (10 μM) and Pb²⁺ (0 - 2 equiv.) in CH₃CN/0.01 M PBS buffer (v/v, 1:1, pH 7.4).

5. Job's Plot

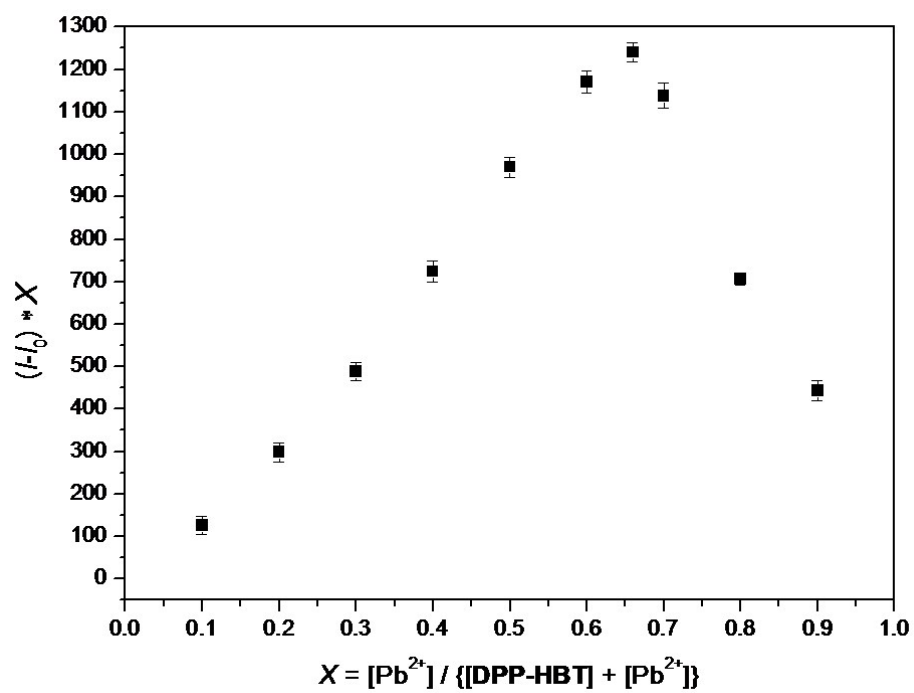


Figure S2. Job's plot for **DPP-HBT** and Pb^{2+} in $\text{CH}_3\text{CN}/0.01 \text{ M PBS}$ buffer (v/v, 1:1, pH 7.4), λ_{ex} : 475 nm.

6. Binding constants

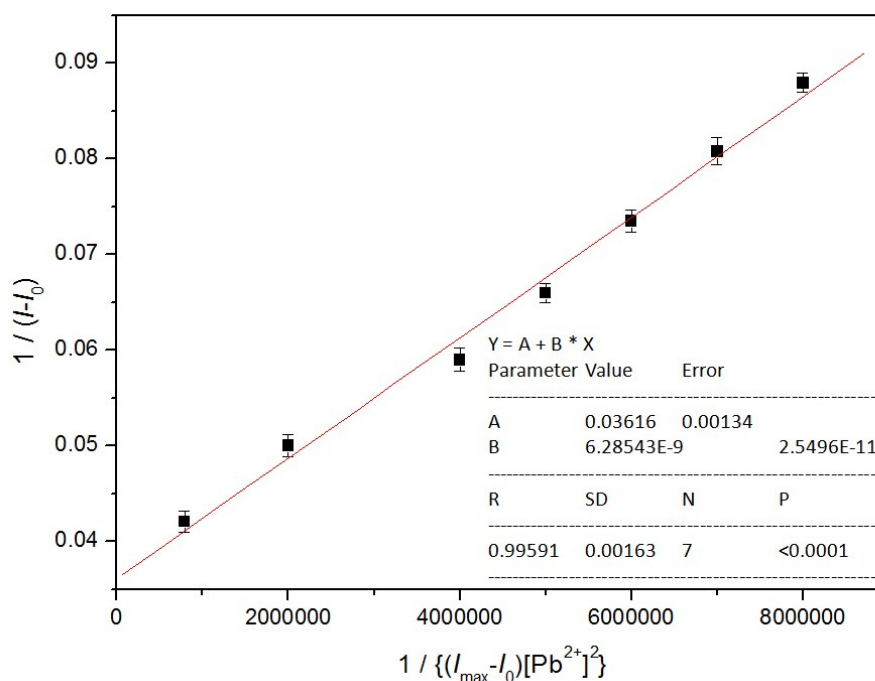


Figure S3. Benesi–Hildebrand plot of probe **DPP–HBT** (10 μM) using 1:2 stoichiometry for association between probe and Pb^{2+} , λ_{ex} : 475 nm..

The binding constants were calculated from the spectral titration data by Benesi–Hildebrand equation:

$$\frac{1}{I-I_0} = \frac{1}{K (I_{\text{max}}-I_0) [\text{Pb}^{2+}]^2} + \frac{1}{I_{\text{max}}-I_0}$$

Where, I_0 was the fluorescence intensity of probe **DPP–HBT**, I the fluorescence intensity obtained with Pb^{2+} , I_{max} the fluorescence intensity obtained with excess amount of Pb^{2+} , K the association constant, $[\text{Pb}^{2+}]$ the concentration of Pb^{2+} added. K was calculated by dividing intercept with slope from the B–H plot by considering 1:2 binding mode between probe **DPP–HBT** and Pb^{2+} . Linear fitting of the titration profiles resulted in a good linearity (correlation coefficient was over 0.996) (Fig. S3), which strongly supported the 1:2 binding stoichiometry of probe **DPP–HBT**, and the binding constant was calculated to be $1.59 \times 10^8 \text{ M}^{-2}$ for probe **DPP–HBT**.

7. Determination of detection limit of Pb²⁺

The detection limit was calculated based on the fluorescence titration. To determine the S/N ratio, the emission intensity of **DPP-HBT** (10 μ M) without Pb²⁺ was measured by 10 times and the standard deviation of blank measurements was determined. Under the present conditions, a good linear relationship between the fluorescence intensity and Pb²⁺ concentration could be obtained in the 0-0.7 μ M (correlation coefficient was 0.9927). The detection limit is then calculated with the equation: detection limit = $3\sigma/k$, where σ is the standard deviation of blank measurements; k is the slope of linear calibration curve. The detection limit was measured to be 0.23 nM at S/N = 3.

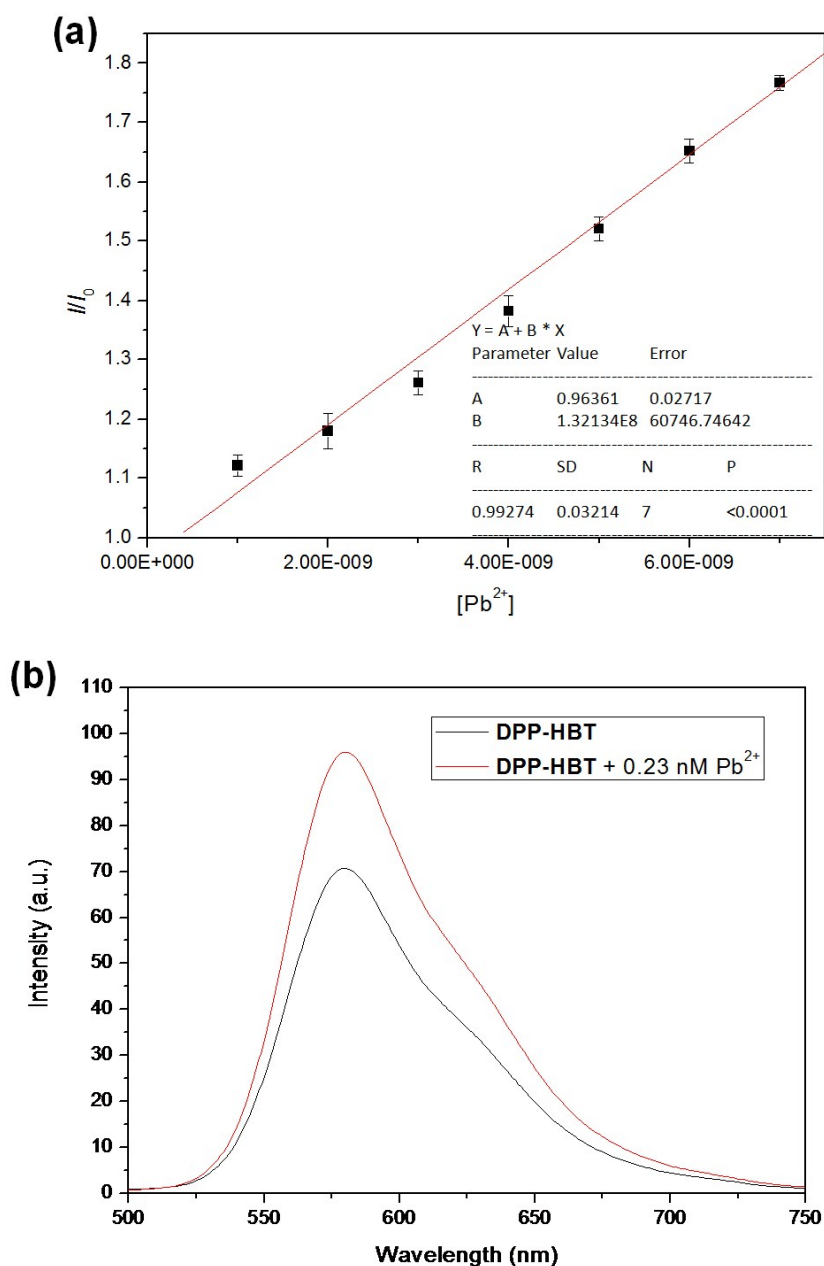


Figure S4. (a) Fluorescence changes of **DPP-HBT** (10 μ M) upon addition of Pb²⁺. (b) Fluorescence spectra of **DPP-HBT** (10 μ M) in the presence of Pb²⁺ (0.23 nM) in CH₃CN/0.01 M PBS buffer (v/v, 1:1, pH 7.4) (λ_{ex} : 475 nm).

8. Time-dependent fluorescence changes of DPP-HBT with Pb²⁺

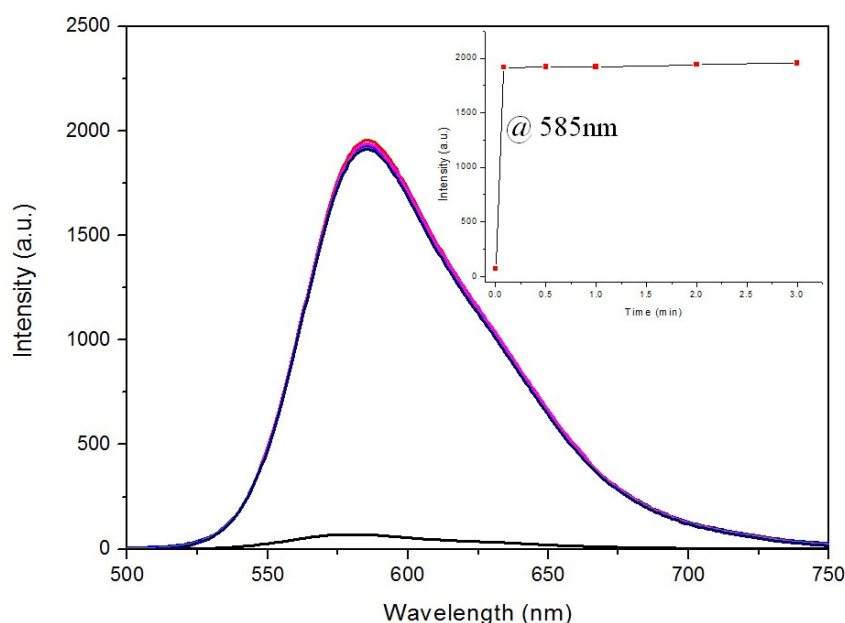


Figure S5. Time-dependent fluorescence spectral changes of **DPP-HBT** (10 μ M) upon addition of 2 equiv. of Pb²⁺ in CH₃CN/0.01 M PBS buffer (v/v, 1:1, pH 7.4), λ_{ex} : 475 nm. Inset: time dependent fluorescence intensity changes (at 585 nm) of probe **DPP-HBT** with Pb²⁺.

9. The fluorescence intensity changes of DPP-HBT in the presence of Pb²⁺ ions and EDTA

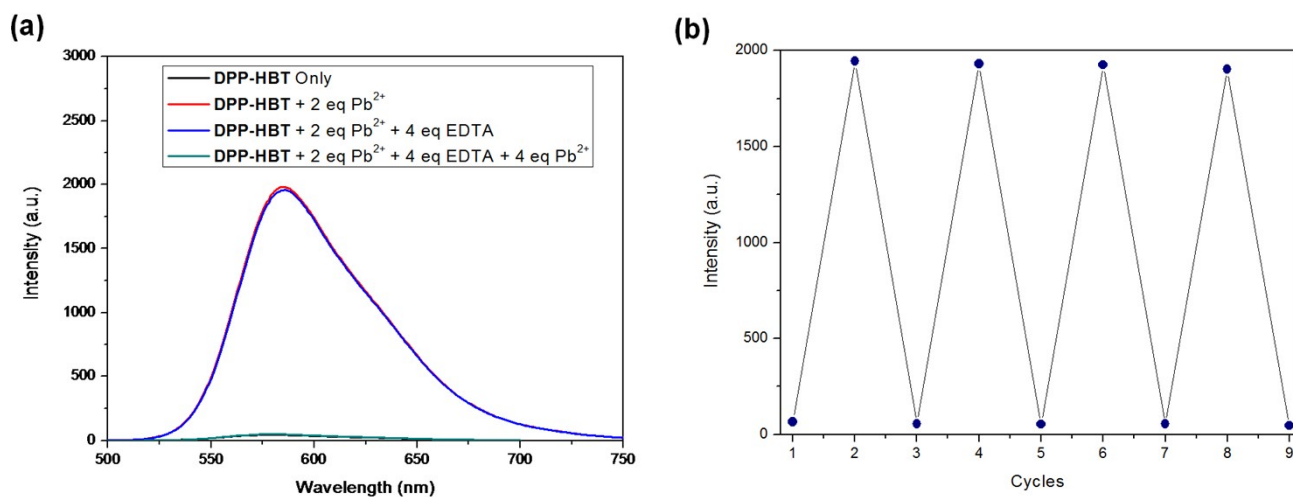


Figure S6. (a) Fluorescence intensity changes of **DPP-HBT** (10 μ M) in CH₃CN/0.01 M PBS buffer (v/v, 1:1, pH 7.4) at excitation at 475 nm after addition of 2 equiv. Pb²⁺, 2 equiv. Pb²⁺+ 4 equiv. EDTA and 2 equiv. Pb²⁺+ 4 equiv. EDTA+ 4 equiv. Pb²⁺, respectively. (b) Stepwise complexation/decomplexation cycles carried out in CH₃CN with **DPP-HBT** and Pb²⁺ ion.

10. Effect of pH

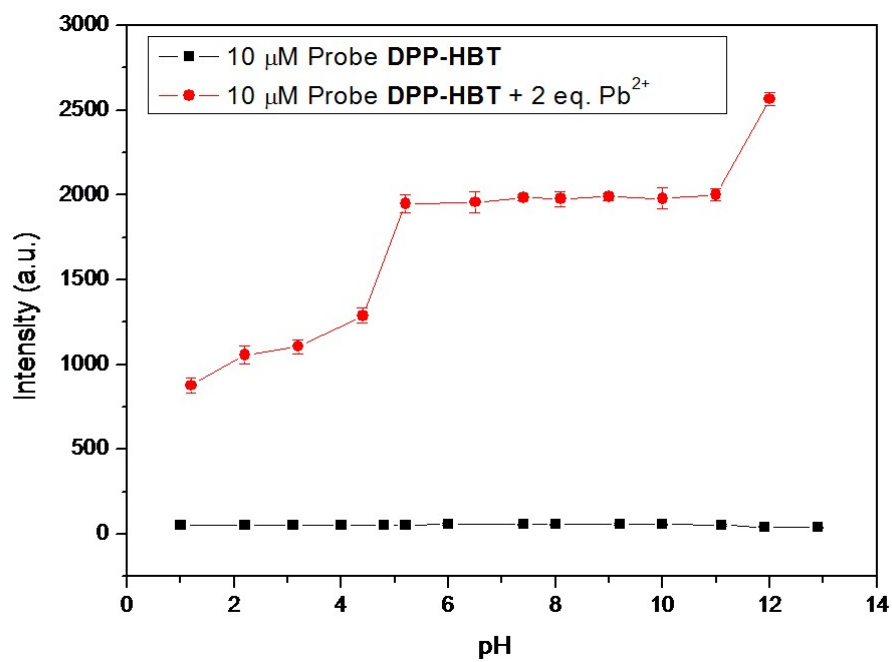


Figure S7. Effect of pH on the fluorescence intensity of **DPP-HBT** (10 μM) in $\text{CH}_3\text{CN}/0.01\text{ M PBS}$ buffer (v/v, 1:1) in the absence (black dot) and presence of Pb^{2+} (red dot). (λ_{ex} : 475 nm).

11. Cytotoxicity assay of DPP-HBT

In vitro cytotoxicity was measured by using the colorimetric methyl thiazolyl tetrazolium (MTT) assay against human lung adenocarcinoma (A549) cells. A549 Human Lung Adenocarcinoma cell lines were grown in DMEM supplemented with 10% FBS (fetal bovine serum) in an atmosphere of 5 % CO₂ at 37 °C. Cells were seeded onto 96-well tissue culture plates in presence of 500 μ L DMEM supplemented with 10% FBS (fetal bovine serum) in an atmosphere of 5 % CO₂ at 37 °C for 24 h and then incubated for 24 h in presence of **DPP-HBT** at different concentrations (10-100 μ M). Then, 20 μ L 3-(4,5-dimethylthiazol-2-yl)-2,5-diphenyltetrazolium bromide MTT (5 mg/mL) was added to each well and incubated for 4 hours. Next, violet formazan crystals were dissolved in 100 μ L of DMSO. The absorbance of solution was measured at 570 nm using microplate reader. The cell viability was determined by assuming 100 % cell viability for cells without **DPP-HBT**.

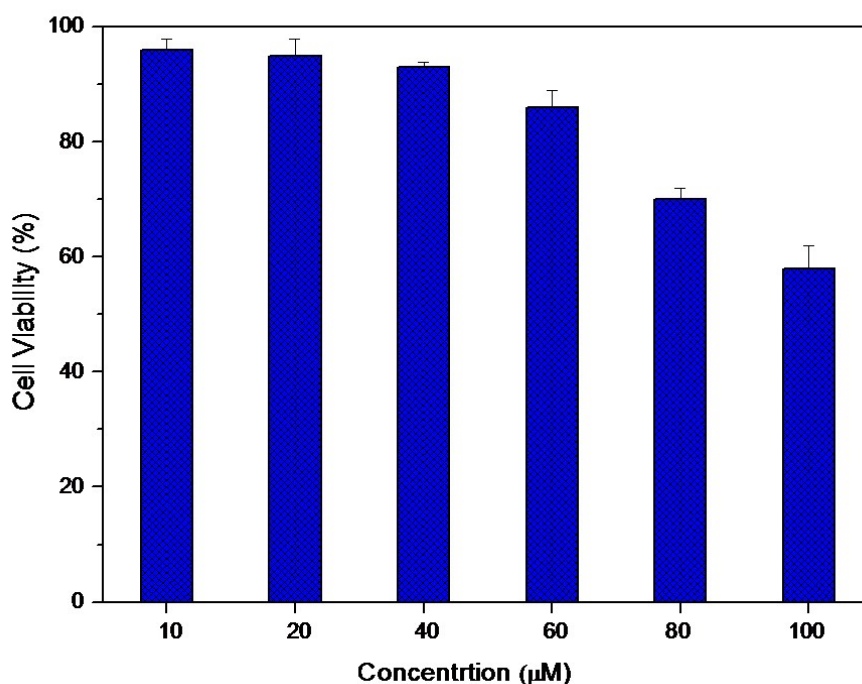


Figure S8. Cell viability of **DPP-HBT** at different concentrations against A549 cells after 24 h incubation.

12. ^1H and ^{13}C NMR of DPP-HBT

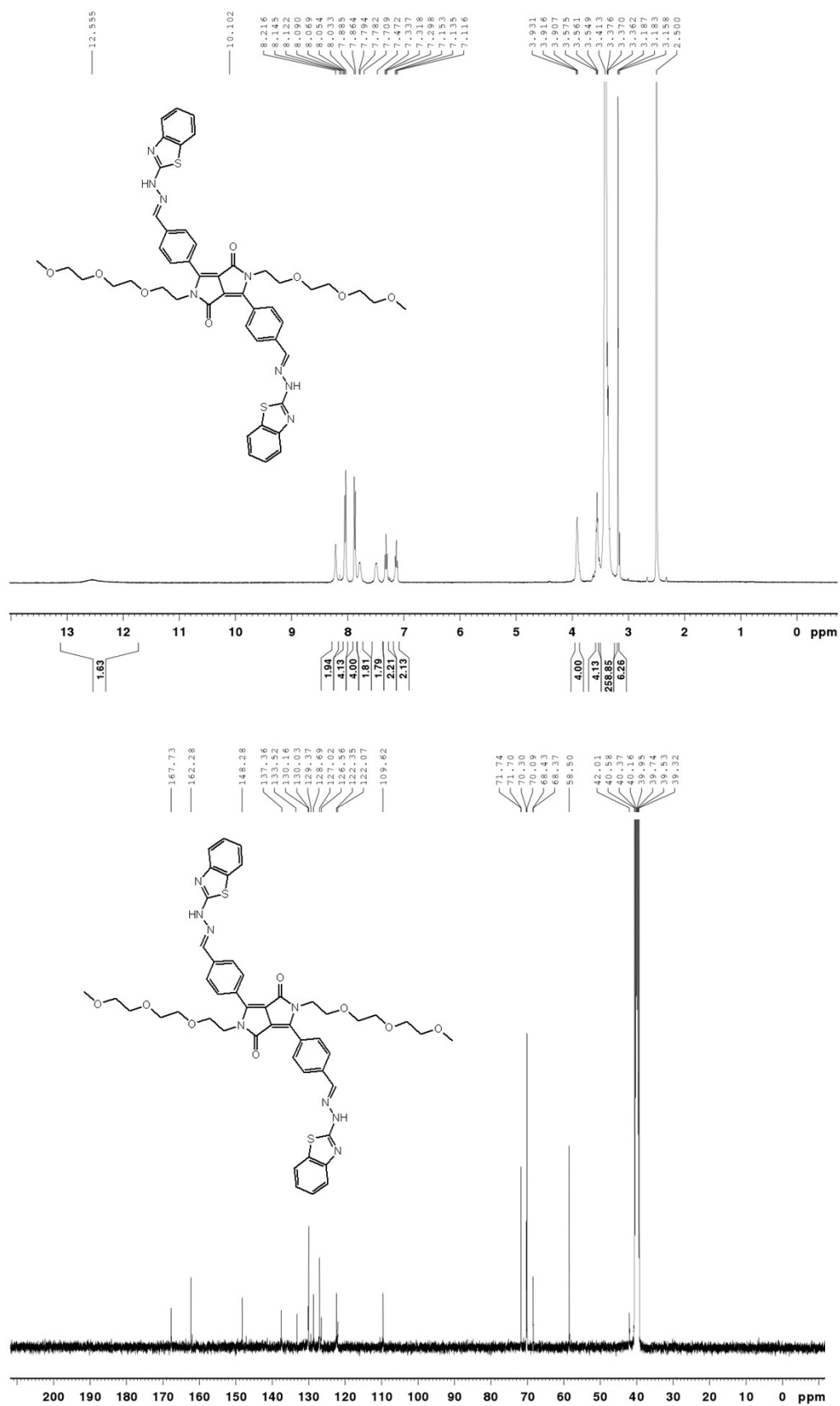


Figure S9. ^1H NMR and ^{13}C NMR spectrum of DPP-HBT (DMSO- d_6 , 400 MHz).

13. Comparison of the present probe **DPP-HBT** and already available Pb²⁺ probes

The detection limit of compound **DPP-HBT** for Pb²⁺ was 2.3×10^{-10} M (Table S1, entry 19), much lower than that of existing organic small molecule probes (Table S1, entries 10–18). These results demonstrated that compound **DPP-HBT** could be used as a high sensitivity probe for Pb²⁺ ions detection.

Table S1. Comparison of the present probe with existing Au³⁺ probes

entry	cell test	the type of probe	LOD	reference
1	not mentioned	nano-material	1.0×10^{-10} M	<i>ACS Appl. Mater. Interfaces</i> , 2014 , 6, 2568–2575.
2	CAL-27 cells	nano-material	1 nM	<i>Analyst</i> , 2015 , 140, 5634–5639.
3	not mentioned	nano-material	50 mg L ⁻¹	<i>Analyst</i> , 2012 , 137, 760–764.
4	not mentioned	nano-material	20 nM	<i>Anal. Methods</i> , 2014 , 6, 9073–9077.
5	not mentioned	nano-material	2 nM	<i>Microchim Acta</i> , 2015 , 182, 695–701.
6	human serum	DNA	22.8 pM	<i>Biosensors and Bioelectronics</i> , 2013 , 43, 231–236.
7	not mentioned	peptide	0.6 nM	<i>Biosensors and Bioelectronics</i> , 2015 , 68, 225–231.
8	not mentioned	quantum dots	9 pM	<i>Chem. Commun.</i> , 2013 , 49, 10599–10601.
9	not mentioned	quantum dots	0.006 nmol L ⁻¹	<i>Journal of Hazardous Materials</i> , 2013 , 250–251, 45–52.
10	not mentioned	organic small molecule	2 ppb	<i>Anal. Chem.</i> , 2013 , 85, 1665–1674.
11	HeLa cells	organic small molecule	1.63×10^{-7} M	<i>Chem. Asian J.</i> , 2014 , 9, 3397–3402.
12	HEK cells	organic small molecule	not mentioned	<i>J. Am. Chem. Soc.</i> , 2006 , 128, 9316–9317.
13	not mentioned	organic small molecule	1.32×10^{-8} M (2.7 μg L ⁻¹)	<i>J. Org. Chem.</i> , 2009 , 74, 4787–4796.
14	not mentioned	organic small molecule	4.64×10^{-6} M	<i>J. Org. Chem.</i> , 2011 , 76, 939–947.
15	not mentioned	organic small molecule	6.3×10^{-7} M	<i>J. Fluoresc.</i> , 2013 , 23, 503–508.
16	not mentioned	organic small molecule	0.49 μM	<i>J. Fluoresc.</i> , 2014 , 24, 19–26.
17	not mentioned	organic small molecule	not mentioned	<i>J. Fluoresc.</i> , 2015 , 25, 557–561.
18	not mentioned	organic small molecule	2.7 μg L ⁻¹	<i>Org. Lett.</i> , 2008 , 10, 41–44.
19	A549 cells	organic small molecule	0.23 nM	Present work